COMPARISON OF CLASSICAL TO H∞-NORM OPTIMAL ROBUST AUTOPILOT DESIGN

B.J.E. Misgeld, A. Reindler and T. Kuhn
Diehl BGT Defence
88662 Überlingen
Germany

ABSTRACT

Classical missile autopilot design methods are based on the linearised airframe, for which an accurate model of the aerodynamics is necessary. In order to cope with nonlinear and time-varying dynamics, the controller is scheduled, dependent on flight conditions. This paper compares such a classically tuned controller to a modern robust control approach. The classical controller is thereby taken from an industrial application and is tuned, using linear quadratic optimal and loop-shaping techniques. Stability is guaranteed over a certain range of nominal models, containing for example unstable and stable airframes. In comparison to that, a robust norm optimal H∞-controller is designed using loop-shaping methods, and tuned for robust stability with the mixed sensitivity constraint. Airframe, mass and time-delay uncertainties are modelled as uncertainties. Classical and norm optimal controllers are compared in linear models and with a detailed and validated nonlinear six degrees of freedom model. The presented approach eliminates the need of an extensive design process, while at the same time robustness can be guaranteed over the whole flight envelope.

1. INTRODUCTION

Automatic missile control systems have to cover a wide operating range, depending on the flight envelope of the missile. In general, one linear controller cannot guarantee stability and the desired control performance over the whole operating range. Therefore the controller has to be adapted to the changing plant dynamics, which is done by gain scheduling. The parameters of the linear controller are changed as a function of flight operating conditions. The classical autopilot design process can be described as follows. First, the airframe is linearised at certain suitable operating points. The controller is designed and tuned at each operating point with the linear airframe, assuming uncoupled roll, pitch and yaw channels. Thereafter, cross-path gains are introduced to the control structure to compensate aerodynamic coupling. The parameters of the autopilot are finally gain scheduled, depending on the operating conditions, used for the linearisation of the airframe. Certain known difficulties arise in the classical design process. The aerodynamic parameter contain uncertainties and are often poorly known. Furthermore, it is sometimes necessary to calculate linear controllers over hundreds of operating points, facing strongly varying plant dynamics. The controller has to guarantee the required performance, that is the stabilisation of the missile and the fast response to acceleration commands, while mass/inertia, thrust profile and control actuating system uncertainties, and a partially unstable airframe may occur. Despite these critical issues the classical control approach has worked well in many technical applications. However, the classical autopilot design process may be expensive and require specific background knowledge. Furthermore, since stability is mostly guaranteed in terms of classical gain and phase margins, even small changes, like mass/inertia or motor properties may require a new stability determination and a retuning of the controllers.

With the introduction of robust control to missile systems in the 1980s, methods, like H∞ design or μ-synthesis were provided, that can guarantee stability and performance in face of exogenous disturbances, namely uncertainties. Robust missile control systems were successfully developed [4],[5], and [6], where different model uncertainties, like actuating system, airframe and mass/inertia were taken into the design.

In this paper, the longitudinal control system for a ground to ground missile is retuned to guarantee control stability and performance. The reason for the retuning of the autopilot are the strongly changed mass/inertia properties, due to an exchanged missile payload. At the same time the classical control approach is compared to a new robust H∞-loop-shaping controller design.

2. SYSTEM MODELLING

The nonlinear missile dynamics are linearised at a certain operating point and the coupling between roll, pitch and yaw motion is neglected. Linear control techniques are then applied to the longitudinal model, where the controller is used for the longitudinal and lateral plane. The controller consists of the classical inner rate feedback loop, for stabilisation of the missile and damping of pitch oscillation. The outer-loop consists of an acceleration feedback for reference tracking of guidance acceleration signals. The linearised longitudinal motion can be described by a second order one input-two output state space model

$$\begin{aligned} \begin{bmatrix} \dot{q} \\ \dot{\alpha} \end{bmatrix} &= \begin{bmatrix} M_q & M_\alpha \\ 1 & Z_\alpha \end{bmatrix} \begin{bmatrix} q \\ \alpha \end{bmatrix} + \begin{bmatrix} M_\eta \\ Z_\eta \end{bmatrix} \eta \\ \begin{bmatrix} q \\ a_z \end{bmatrix} &= \begin{bmatrix} 1 & 0 \\ Z_q & Z_\alpha \end{bmatrix} \begin{bmatrix} q \\ \alpha \end{bmatrix} + \begin{bmatrix} 0 \\ Z_\eta \end{bmatrix} \eta \end{aligned}, \quad (1)$$

where η is the commanded pitch deflection (pitch elevator), q is the pitch rate, α is the angle of attack and a_z is the acceleration in z-direction. The derivatives in (1) depend on the operating point (trimmed aerodynamic) and are defined by [1]

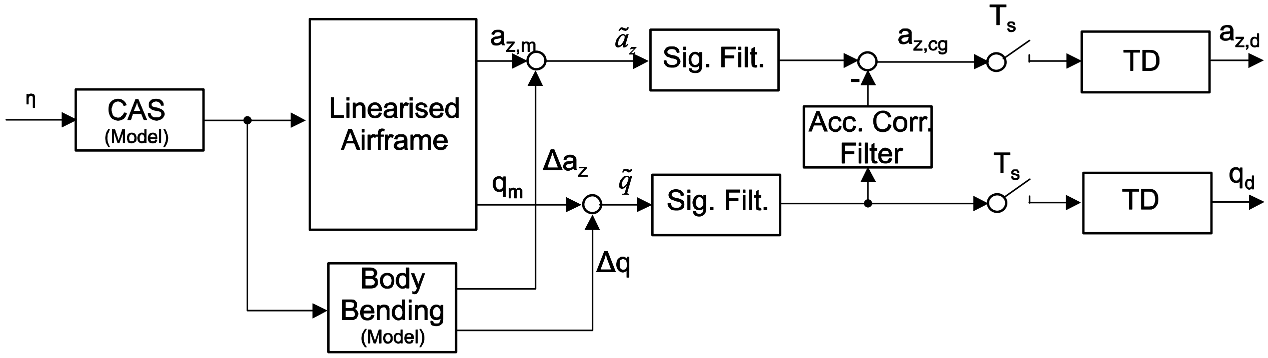

FIG 1. Full linear model used for linear analysis and stability determination (with time-delay TD).

$$M_\alpha = \bar{q}\frac{Sl_r}{I_{yy}}C_{m\alpha}$$

$$M_q = \bar{q}\frac{Sl_r}{I_{yy}}\frac{l_r}{V_0}(C_{mq}+C_{m\dot{\alpha}})$$

(2) $$M_\eta = \bar{q}\frac{Sl_r}{I_{yy}}C_{m\eta}$$

$$Z_\alpha = -\bar{q}\frac{S}{mV_0}(C_W + C_{A\alpha})$$

$$Z_\eta = -q\frac{S}{mV_0}C_{A\eta}$$

The controller is tuned with the second order model (see Section 3), where stability analysis were conducted using the full order linear model, see Fig. 1. For the full order model, the longitudinal pitch model (1) was extended with the dynamics of the control actuating system (CAS). The CAS was modelled as a second order state-space model with damping ζ and cut-off frequency ω_0. The structural vibrations due to aeroelastic effects were modelled as a very low damped second order state space model, with resonance frequency ω_{bb} and damping D_{bb}. However, only the first vibrational eigenmode was modelled in the space model

(3)

$$\begin{bmatrix}\dot{x}_{bb,1}\\ \dot{x}_{bb,2}\end{bmatrix} = \begin{bmatrix}1 & 0\\ -\omega_{bb}^{\ 2} & -2D_{bb}\omega_{bb}\end{bmatrix}\begin{bmatrix}x_{bb,1}\\ x_{bb,2}\end{bmatrix} + \begin{bmatrix}0\\1\end{bmatrix}F_\eta$$

$$\begin{bmatrix}\Delta q\\ \Delta a_z\end{bmatrix} = \begin{bmatrix}0 & -\Phi_{CASROT}\Phi_{IMUROT}\\ -\Phi_{CASDIS}\Phi_{IMUDIS}\omega_{bb}^{\ 2} & -\Phi_{CASDIS}\Phi_{IMUDIS}\end{bmatrix} + \begin{bmatrix}0\\ \Phi_{CASDIS}\Phi_{IMUDIS}\end{bmatrix}F_\eta$$

where Φ_{CASDIS}, Φ_{IMUDIS} and Φ_{CASROT}, Φ_{IMUROT} are the CAS and the inertial measurement unit (IMU) modal displacement and rotation, respectively. The errors in displacement rate and acceleration $[\Delta q \ \ \Delta a_z]^T$ were added to the outputs of the pitch motion state space model (see Fig.1)

(4) $$\begin{bmatrix}\tilde{q}\\ \tilde{a}_z\end{bmatrix} = \begin{bmatrix}q\\ a_z\end{bmatrix} + \begin{bmatrix}\Delta q\\ \Delta a_z\end{bmatrix}.$$

The input force that excites the body bending modes is defined as

(5) $$F_\eta = C_{N\delta}S\bar{q}\eta\,.$$

Since the body bending resonance frequency changes during missile boost phase, it was modelled as a function of MACH number. The measured IMU rate and acceleration signals are filtered by 2nd order notch filters, to damp the body bending resonance frequency and 2nd order low pass filters, which were implemented to reduce high freqency noise effects. The acceleration error due to IMU misplacement was corrected by an acceleration error correction filter, which subtracts the estimated acceleration rate term

(6) $$G_{acc}(s) = l_a\frac{\omega_a^{\ 2}s}{s^2 + 2\zeta_a\omega_a + \omega_a^{\ 2}},$$

where l_a is the lever arm from IMU to centre of gravity. The model was finally discretised and the time-delay for calculation in the flight computer was incorporated. Note, that the pitch dynamics and model filter constants were initialised at each operating point for classical controller design. This is described in more detail in the control section below.

3. CONTROL DESIGN

3.1. Classical Control Design

For classical control design, the missile operating range was divided into n points for the dynamic pressure and m points for the MACH number. This gives a total of n×m operating/linearisation points, where the controller has to be tuned with regard to changed plant dynamics. Angle-of-attack and sideslip angle, but as well variations in the centre of gravity of 25% of the missile calibre were assumed as uncertainties in the design process. That means, that in every operating point the stability analysis with classical gain and phase margins was conducted over the number of uncertain models. When stability conditions, i.e. predefined gain and phase margins were violated, the controller design and stability determination were repeated. A description of the design process follows below. For the inner-rate feedback loop a pole-zero compensator

(7) $$K_{rf}(s) = \frac{k_{pzc}s + z_{pzc}}{s + p_{p\eta}}$$

was applied to the feedback path. The pole of the compensator was placed at the zero of the pitch rate transfer function

(8)

$$G_{q\eta}(s) = \frac{M_\eta s + M_\alpha Z_\eta - Z_\alpha M_\eta}{s^2 - (Z_\alpha + M_q)s + Z_\alpha M_q - M_\alpha(1 + Z_q)}$$

The gain of the pole zero compensator and the zero were calculated as the solution of the optimal linear-quadratic state feedback regulator problem, with the state space model (1)

(9) $$J(u) = \int_0^\infty (\mathbf{x}^T\mathbf{Q}\mathbf{x} + \mathbf{u}^T\mathbf{R}\mathbf{u} + 2\mathbf{x}^T\mathbf{N}\mathbf{u})dt\,,$$

where the minimisation of the state feedback $\mathbf{u} = -\mathbf{K}\mathbf{x}$ leads to the associated Algebraic Matrix Riccati equation and the closed-loop eigenvalues $\lambda_i(\mathbf{A} - \mathbf{B}\mathbf{K})$.

For the outer-loop acceleration feedback design, the inner rate-loop was closed and a PI-controller of the form

(10) $$PI_{af}(s) = \frac{k_p s + k_i}{s}$$

was tuned using classical loop-shaping design. At the end of inner and outer loop design, the control circuit was discretised and time-delays are incorporated.

The classical stability margins were checked again and, if violated, the design procedure was repeated. The process could be partly automated but it is still a computational intensive and time consuming method. However, at the end one ends up with an inner-loop rate compensator and an outer-loop acceleration reference tracking controller for each of the n×m MACH/dynamics pressure operating points.

3.2. Robust Control Design

For robust inner and outer loop controller design, the following strategy was chosen. The operating range was divided into n points for dynamic pressure, where the MACH condition, in contrast to the classical approach, is assumed as additional uncertainty. In a first step, the system uncertainty was modelled for the control design process. Uncertainty was modelled for each feedback loop as unstructured multiplicative uncertainty $l_m(s)$, where the family of uncertain plants $G_p(s)$ is described by

(11) $G_p(s) = \tilde{G}(s)(1 + l_m(s))$,

with the nominal plant $\tilde{G}(s)$. The multiplicative uncertainty for the family of plants Π is then defined by

(12) $$\Pi = \left\{ G_p(s) : \frac{\left|G_p(s) - \tilde{G}(s)\right|}{\left|\tilde{G}(s)\right|} \le \bar{l}_m(s) \right\},$$

where $\bar{l}_m(\omega) \ge |l_m(s)|$ is the unstructured multiplicative uncertainty bound [2]. The multiplicative uncertainty bound for the airframe was modelled as a second order complex frequency weight,

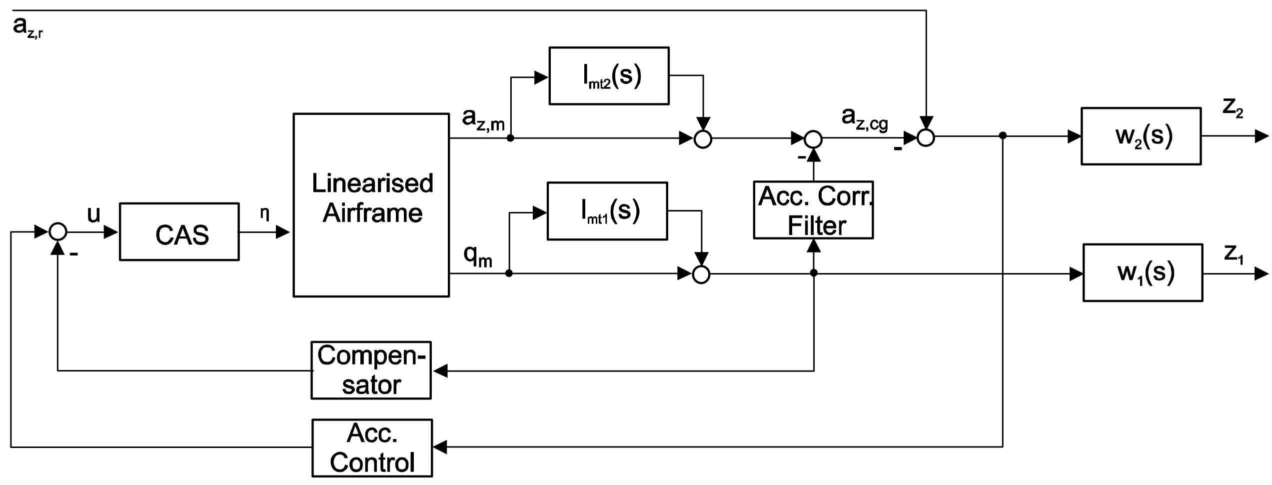

FIG 2. Augmented plant for loop-shaping H_∞-synthesis.

(13) $l_{m1}(s) = k_{m1} \dfrac{(\alpha_{m1} s + 1)^2}{(\beta_{m1} s + 1)^2}$,

with gain k_{m1} and time constants α_{m1} and β_{m1}. Note that the uncertainty $l_{m1}(s)$ was modelled for each , the rate and the acceleration loop, to $\mathbf{l}_{mm}(s) = [l_{m11}(s)\ l_{m12}(s)]^T$. For the time-delay uncertainty T_δ follows the frequency dependent uncertainty to [2]

(14) $l_{m2}(s) = e^{-sT_\delta} - 1$,

which can be described as

(15) $|l_{m2}(s)| = \begin{cases} 2\sin\dfrac{\omega T_\delta}{2} & \forall \omega \le \dfrac{\pi}{T_\delta} \\ 2 & \forall \omega \ge \dfrac{\pi}{T_\delta} \end{cases}$.

The uncertainty was modelled with a first order frequency weighting

(16) $\overline{l}_{m2}(s) = k_{m2} \dfrac{\alpha_{m2} s + 1}{\beta_{m2} s + 1}$.

Finally, the CAS uncertainty was modelled with a frequency weighting of structure (16). All three multiplicative uncertainties were lumped together to

(17) $\mathbf{l}_{mt}(s) = \mathbf{l}_{mm}(s) \cdot l_{m2}(s) \cdot l_{m3}(s)$.

The control performance was specified with a frequency dependent weighting for rate compensation and acceleration tracking $\mathbf{w}(s) = [w_1(s)\ w_2(2)]$. For the inner-loop rate compensation the lead-lag frequency weight $w_1(s)$ was chosen of structure (7). Gain, bandwidth and lag pole were adopted from the classical rate compensator in the mean MACH range at a certain dynamic pressure. In the same way the frequency was chosen for the outer-loop acceleration feedback circuit. For this case, a frequency weight with integral gain and of structure (10) was adopted to the gains of the classical PI-acceleration loop controller in the mean dynamic pressure range. For the H_∞-loop shaping approach, the nominal model was extended with the loop-shaping weightings (see FIG 2). With the sensitivity function $\mathbf{S}(s)$, consisting of the closed loop nominal plant with acceleration filter correction, the requirement for nominal performance is [3]

(18) $\|\mathbf{w}(s)\mathbf{S}(s)\|_\infty < 1$.

Robust stability is guaranteed if

(19) $\|\mathbf{T}(s)\mathbf{l}_{mt}(s)\|_\infty < 1$,

where $\mathbf{T}(s)$ is the complementary sensitivity function, defined for the plant given in FIG 2. The robust controllers for rate compensation and acceleration reference tracking were designed with the mixed sensitivity constraint for robust performance

(20) $\|\mathbf{G}_{\mathbf{w},\mathbf{z}}(s)\|_\infty = \sup_{\omega\in\Re} |\mathbf{G}_{\mathbf{w},\mathbf{z}}(s)| < 1$,

where **w** corresponds to the exogenous inputs, **z** to the regulated outputs and the transfer function $\mathbf{G}_{\mathbf{w},\mathbf{z}}(s)$ is

(21) $\mathbf{G}_{\mathbf{w},\mathbf{z}}(s) = \begin{bmatrix} \mathbf{w}(s)\mathbf{S}(s) \\ \mathbf{T}(s)\mathbf{l}_{mt}(s) \end{bmatrix}$.

For the numerical solution of the robust control problem above, the MATLAB Robust Control Toolbox was used. An 8th order controller was calculated for the inner-loop compensator and for the outer-loop acceleration circuit. Note however, that the robust controller was calculated with the plant given in FIG 2. The plant lacks body bending and signal conditioning. Body bending and signal conditioning were simply neglected to prevent the controller order from rising another six dimensions. The full model including signal conditioning and body bending was used for the linear analysis.
The robust control design for the inner-loop compensator and a partially stable airframe was slightly different to the approach presented above. A partially unstable airframe can occur during missile boost phase, for medium to high incidences. For the design of the inner-loop compensator, which has to stabilise the missile, airframe uncertainty of stable and unstable missiles was modelled as inverse uncertainty [3]

(22) $G_p(s) = \tilde{G}(s)(1 + w_{mI}(s)\Delta(s))^{-1}$

in which $w_{mI}(s)$ is the multiplicative inverse uncertainty and $\Delta(s)$ is a frequency dependent weighting, used for the realisation of the uncertainty. The inner loop rate compensator was then tuned with multiplicative uncertainty using the robust stability theorem (19) and the robust performance theorem for robust stability with inverse multiplicative uncertainty [3]

(23) $\|w_{mI}(s) S_{IL}(s)\|_\infty < 1$,

where $S_{IL}(s)$ is the sensitivity transfer function for the inner-loop. With the inner loop closed, and the so stabilised airframe, the outer-loop design is the same as described above. Note however, that the resulting inner-loop compensator, that stabilises stable and unstable airframes is similar to the LQR-compensator (see above).

4. LINEAR ANALYSIS

The full linear model, given in FIG 1, was extended with rate compensation and acceleration feedback control. The stability of the control loop was then determined by the classical gain and phase margins in frequency responses. To include uncertain models to the stability analysis, the airframe was linearised for each MACH/dynamic pressure combination with centre of gravity uncertainty of ± 0.25 missile calibres in x-direction and zero and maximum incidence. This gives a total of four uncertain sample models at each operating point. Note however, that the H_∞-rate compensation and acceleration tracking controllers were designed for the whole MACH operating range, which means that stability analysis was conducted over $4 \times m$ uncertain models.
When comparing the stability margins of the classical to the robust control approach, the robust controller provided stability over the uncertain models and the whole MACH range at a fixed dynamic pressure (meaning varying velocity and air density over a range of altitudes). Since the classic controller is scheduled two-dimensionally with regard to every MACH/dynamic pressure operating condition the absolute stability margin was superior compared to the robust approach. An example for the stability differences is given for a certain dynamic pressure in TAB 1. For classical and robust control the worst case stability margins are given.

TAB 1. Worst case gain- (GM) and phase-margins (PM) for the inner- (IL) and outer-loop (OL) compensated plant at a certain flight condition.

	GM IL	PM IL	GM OL	PM OL
Classical	9.1 dB	47.1°	6.7 dB	51°
H_∞-con.	3.8 dB	32.5°	19.6 dB	63.3°

The lower stability margins of the inner-loop compensator circuit can be attributed to the strongly changing gain and resonance frequency of the pitch transfer function. This can also be seen from FIG 3, where the robust inner-loop compensated frequency response at an example flight condition is shown over all linearised models, containing uncertainties and different MACH conditions.

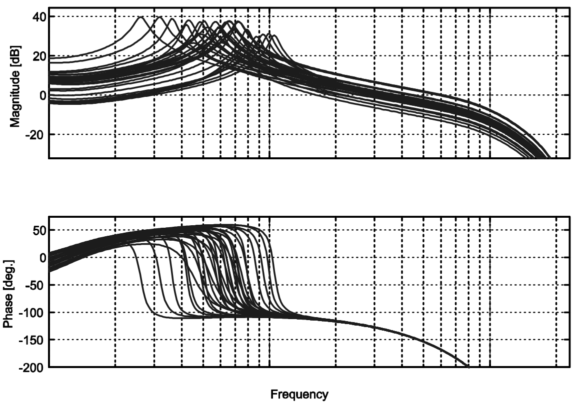

FIG 3. Compensated inner-loop rate circuit with robust compensator at an example flight condition, over MACH range linearised models containing uncertainty.

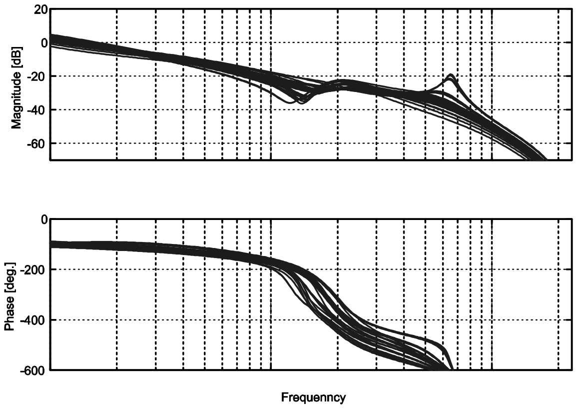

FIG 4. Compensated outer-loop acceleration circuit with robust controller, over MACH range linearised models containing uncertainty.

The corresponding outer-loop compensated control circuit, with the inner-loop closed is shown in FIG 4 for the robust controller. The H_∞-controller gain is similar to the classical PI-controller, but is reduced significantly at higher frequencies to damp higher resonance frequencies, lever arm correction filter and uncertainty effects. Since the robust controller is not gain scheduled dependent on MACH number, it provides a higher gain margin over the MACH operating points. The lower gain margin of the classical controller (TAB 1) is due to the tuning to each of the m MACH operating conditions. The classical outer-loop PI-controller comprises more gain and a higher bandwidth at certain MACH operating conditions. This will become clear, when directly comparing the time domain responses of classical and H_∞-controller.

FIG 5 shows the timeline responses of the inner-loop rate compensated circuit to a step response. The figure corresponds to a higher missile velocity and a dynamic pressure in the mid range, at an respective altitude of about 18km.

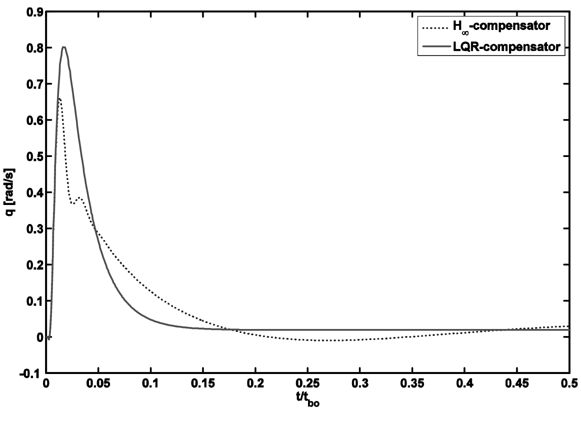

FIG 5. Compensated rate-loop step response an example operating point of high velocity and medium dynamic pressure with CG_X uncertainty of +0.25 calibres.

In addition to the MACH uncertainty for the H_∞-controller, uncertainty of +0.25 calibres for the x-centre of gravity in tail direction was assumed in the model linarisation. The H_∞-controller shows a slightly underdamped behaviour and a slower stabilisation response. The good stabilisation performance of the LQR-rate compensator is due to the adaptation of the lead-lag compensator to changed resonance frequency of pitch oscillation. In the next step, the compensated rate loop was closed and acceleration feedback was applied to the full linear model (FIG 1). The step response of the acceleration reference tracking control loop is shown in FIG 6.The H_∞-controller shows again a slower response, compared to the classical outer-loop PI-controller. This is because of the lower bandwidth of the robust control loop in order to satisfy robust stability in face of modelled uncertainties. The slightly undamped resonance frequencies of the classical controller can be seen after step onset.

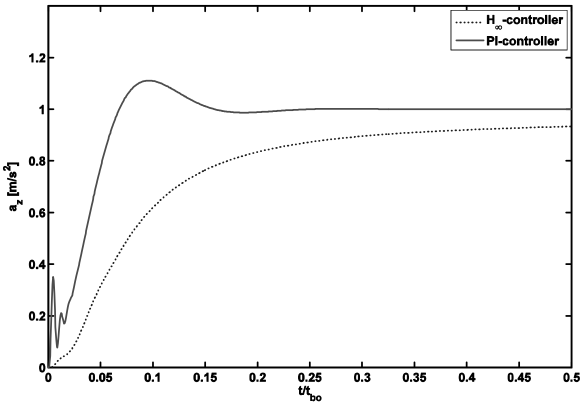

FIG 6. Acceleration reference step response at high velocity and medium dynamic pressure with CG_x uncertainty of +0.25 calibres.

The linear analysis shown for the dynamic pressure example was repeated over the other dynamic pressure operating points. Similar results to those, presented in the examples above were obtained. Controllers obtained by the robust approach were stable over all sampled models at different MACH operating points and containing uncertainties. However, the stability in terms of classical stability margins was in general more critical in the inner-loop rate circuit. Good stability results could be observed in the outer-loop acceleration circuit at the cost of a reduced control bandwidth.

5. NONLINEAR SIMULATION

After linear evaluation, the controllers were tested in a detailed and validated six-degrees-of-freedom model in nonlinear simulation. The model consisted of full missile aerodynamics (table-lookup), truth, thrust, autopilot and atmosphere models. Truth model equations were set up for the flat, non-rotating earth [8]. Mass and inertia matrix were changed as a function of time during boost phase. Body bending and CAS dynamics were included to the model. The classical and the robust autopilot were tested in different operating ranges in acceleration step responses and disturbance rejection test series. For that, the initial values of the model were initialised with trimmed height and aerodynamics belonging to a certain MACH dynamic pressure operating condition. Simulations were repeated with applied x-axis centre of gravity uncertainty and for maximum allowed acceleration commands (determined by the guidance command limiter).

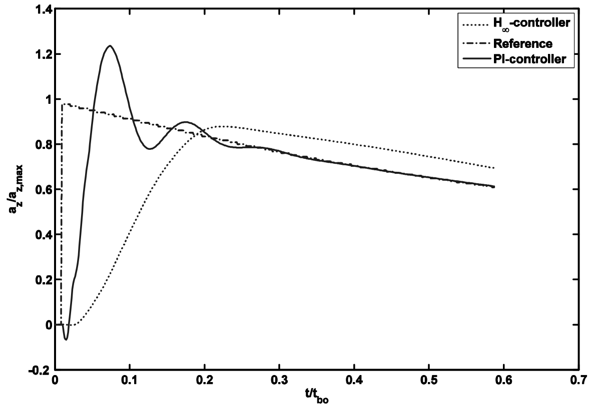

FIG 7. Acceleration reference step response at a lower velocity/medium dynamic pressure, with CG_x uncertainty of +0.25 calibres.

During all simulations stable results were obtained with the H_∞-controllers. FIG 7 shows an example of an acceleration step response at a lower velocity and a medium dynamic pressure, with a corresponding altitude of about 2.8 km. Uncertainty for the x-centre of gravity (0.25 calibres) was included to the model. The acceleration reference step was chosen to the be the maximum acceleration of the guidance command limiter. The results look similar to those observed in linear analysis. Note however, that the overshoot of the classical PI-controller has no direct connection with the classical gain and phase margin results made in the linear analysis. The resulting rate control response to the acceleration step of FIG 7 is shown in FIG 8.

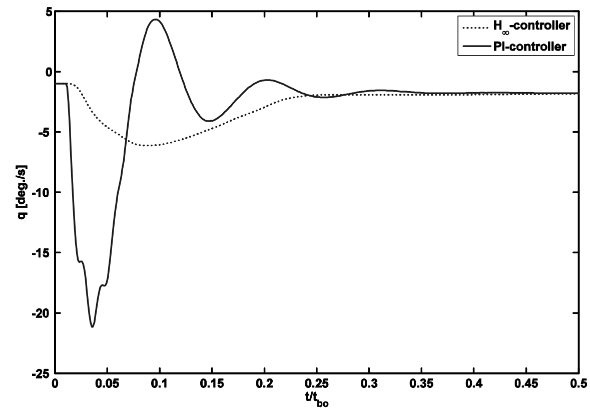

FIG 8. Rate response to the accceleration step command at at a lower velocity/medium dynamic pressure, with CG_x uncertainty of +0.25 calibres.

The higher rate amplitude response of the classical controller is due to the faster acceleration control loop response, given in FIG 7. Step responses, like those shown in FIG 7 and FIG 8 were repeated in other operating areas with centre of gravity uncertainty and maximum possible acceleration reference. Obtained results looked similar to those presented above. The classical controller showed superior control performance over all operating points, where the damping of the inner-loop rate circuit is acceptable. The acceleration response of the H_∞-controller degrades to slower responses at MACH operating points with lower system gain.

6. RESULTS AND DISCUSSION

A robust autopilot was designed for the full flight envelope of a ground-to-ground missile, using a loop shaping H_∞-control approach. The controller for rate compensation and acceleration tracking was then compared to a classical control approach. The main difference between classical and robust approach is the way in which the controllers are scheduled. In the classical approach, controller parameters are scheduled two dimensionally as a function of MACH number and dynamic pressure. In contrast to that, the robust controllers are scheduled depending on dynamic pressure, where the actual gain scheduling can be easily done using controller conditioning/blending schemes, as presented in [6], [7]. Once the augmented plant, the performance and the uncertainty weight are defined, the straight forward tuning of the controller showed out to be the main advantage of the H_∞-control approach. Furthermore, the uncertainty defined in this approach accounts for mass or inertia changes, where the robust controller guarantees robustness. A new stability determination and retuning of the controller may therefore be avoided on changed mass/inertia properties. Note however, that the frequency dependent multiplicative unstructured uncertainty, used for the modelling of uncertainty, is more conservative in the control approach, compared for example to μ-synthesis. Degrading control performance was therefore observed for the robust controller at some operating points, since controllers are scheduled only over the dynamic pressure operating range. As a result of the robust tuning process two 8^{th} order controllers were calculated at each dynamic pressure operating point. The order of the robust controllers is not considered to be a problem, since, if necessary, order reduction techniques can be applied [9]. On the other hand, the gain scheduled classical lead-lag, PI-controller design shows the superior control performance. This is of because of the two-dimensional adaptation of control parameters to operating conditions, which were assumed as uncertainty in the robust approach. If the controller parameter tuning process can be automated with certain design and tuning constraints or tuned by parameter optimisation [10], the classical design may be endowed with further advantages. The simple interpolation of low order controllers depending on operating conditions saves calculation cost, compared to high order robust controllers undergoing a blending scheme. Furthermore, if a certain gain and phase margin can be guaranteed over all operating points robust stability can be checked with the modelled uncertainty. It is suggested that the control performance of the robust approach can be significantly increased if parametric uncertainty modelling is used in the controller design process. It is further suggested that a further reduction of operating space grid points to reduce the number of designed controllers is possible and will minimise further the design effort. This is subject to ongoing work.

7. LITERATURE

[1] Brockhaus, R.: Flugregelung. Springer-Verlag, Berlin Heidelberg, 1994
[2] Morari, M. and Zafiriou, E.: Robust Process Control. Prentice-Hall International, Inc. Englewood Cliffs N.J., 1989
[3] Skogestad, S. and Postlethwaite, I.: Multivariable Feedback Control, John Wiley and Sons, Chichester, 2005
[4] Reichert, R. T.: Application of H_∞ Control to Missile Autopilot Design, AIAA Guidance, Navigation and Control Conference, Boston, MA, pp. 1065-1072, 1989
[5] Shamma, J. S. and Cloutier, J. R.: Gain-Scheduled Missile Autopilot Design Using Linear Parameter Varying Transformations, Journal of Guidance, Control and Dynamics, 16(2), pp. 256-263, 1993
[6] Buschek, H.: Full Envelope Missile Autopilot Design Using Gain Scheduled Robust Control, Journal of Guidance, Control and Dynamics, 22(1), pp. 115-122, 1999
[7] Hyde, R. A.: H_∞ Aerospace Control Design, Springer-Verlag Berlin Heidelberg New York, 1995
[8] Stevens, B. L. and Lewis, F. L.: Aircraft Control and Simulation, John Wiley and Sons, New Jersey, 2003
[9] Zhou, K., Doyle, J., Glover, K.: Robust and Optimal Control, Prentice Hall, New Jersey, 1996
[10] Kleinwächter, F., Kuhn, T., "Robuste Auslegung strukturfester Flugregler mittels Polvorgabe und Parameteroptimierung", DGLR-Jahrestagung, Friedrichshafen, 2005